



Fluid Dynamics Analysis of Flow through T-junctions and Venturi Meters Using Computational Methods

G Kavin^{1*}, S Vignesh², R Subhasan³, M Shanmugavalli⁴

¹Student, Instrumentation and Control Engineering, Saranathan College of Engineering, Trichy, India.

²Student, Instrumentation and Control Engineering, Saranathan College of Engineering, Trichy, India.

³Student, Instrumentation and Control Engineering, Saranathan College of Engineering, Trichy, India.

⁴Professor, Instrumentation and Control Engineering, Saranathan College of Engineering, Trichy, India.

*Corresponding author

DoI: <https://doi.org/10.5281/zenodo.11050097>

Abstract

In this study, we're examining how water flows through a T-junction and into a Venturi tube via a pipe. We're using a computer program called ANSYS FLUENT 2018.1 to help us understand what's going on. We're interested in how things like the speed of the water and the pressure change as it moves through this system. To do this, we're looking at a few different factors. We're considering the size of the pipe (which is 25 mm in diameter) and how far it is from the T-junction to the outlet of the Venturi tube (which is 350 mm). We're also looking at something called the Reynolds number, which helps us understand how the water behaves at different speeds. I had particularly interested in how turbulent the water flow is. Imagine stirring a cup of water - sometimes it flows smoothly, and other times it gets all choppy. We're studying this turbulence to see how it affects the flow of water in our system. After running the simulations, we found that the T-junction has a different impact on the venturi tube when it comes to the speed of the water and the pressure. However, we noticed that the turbulence in the water stays pretty consistent throughout the system.

Keywords: CFD, Turbulent Flow, Characteristics centerline, T-junction, Venturi meter , Turbulence modeling, Converging-diverging flow, Pressure distribution, Velocity profiles, Flow separation.

1. Introduction

When fluid moves through pipes and ducts, it encounters resistance which affects its flow. In pipes, this resistance is determined by factors such as the roughness of the pipe surface, friction losses, as well as additional losses caused by components like gate valves, ball valves, sudden expansions, and connections such as T-junctions. All these factors influence the velocity, pressure, and other parameters of the flow. There are two primary types of flow within pipes, determined by the aforementioned factors affecting the flow. The first type is known as laminar flow, characterized by fluid passing through smooth layers of laminae, resulting in streamline flow where fluid particles move in parallel lines.

When the flow velocity surpasses a certain threshold, it transitions from laminar to turbulent. In turbulent flow, particle movement becomes erratic and fluctuates both perpendicular and parallel to the mean flow direction. The assessment of Reynolds numbers (Re) is crucial in determining whether the flow within a pipe is laminar or turbulent. Pipe networks heavily rely on components like T-junctions, which are common in water and industrial systems. T-junctions serve to divide the flow from the main pipe into multiple branch streams and to gather flows from two pipes. Ensuring the appropriate sizing of lines requires an accurate assessment of energy losses at junctions, which significantly influences hydraulic calculations and, in certain scenarios, the selection of pumps. Calibrating the Venturi meter in a laboratory, mirroring the installation setup anticipated in the field, is essential for dependable flow measurement. However, the feasibility of this calibration hinges on factors such as the size of the Venturi and the configuration of the piping system.

When employing a Venturi tube for flow measurement, it generates a pressure differential proportional to the flow rate, known as a Venturi meter. These meters gauge flow rate by

assessing the rise in flow velocity and the corresponding pressure drop attributable to the tapered section of the pipe. Venturi flow meters have been utilized by water supply companies for an extended period. An investigation was conducted to evaluate the impact of a tee junction on the flow rate measurement of a Venturi flow meter positioned downstream of the branch. The velocity of water is significantly influenced by the 90-degree angles inherent in the T-junction of the pipe. Moreover, water velocity experiences a notable increase with a reduction in the diameter of the test section, while minimizing the angle of the T-junction can help mitigate energy losses in the pipe.

An investigation was conducted on T-junctions featuring sharp and curved corners. In the main pipe, the loss coefficient remains consistent in both cases, yet it notably decreases in the branch pipe. The study aimed to assess the impact of pipe size and beta values on discharge coefficients by examining different models of flow meters. It was found that the length of straight pipe needed is influenced by the type of upstream fitting of the meter and the ratio of throat to inlet diameter. The precision of a Venturi meter hinges on the length of straight pipe preceding the meter.

2. Methodology

2.1. Description of Venturi Meter

A standard Venturi tube crafted from transparent Epoxy material, calibrated in water with a diameter ratio (β) of 0.6, was obtained from reference [12]. The convergent and divergent angles were fixed at 10.5 and 3.5 degrees, respectively. The length of the inlet cylinder matches the internal diameter of the branch pipe, $D = 25\text{mm}$, while the length of the throat section equals the internal diameter of the throat, $d = 15\text{mm}$. The divergent section measures 82mm in length. The overall length of the Venturi meter is 150mm, with the upstream pipe

extending to 8 times the diameter (8D). Maintaining the Integrity of the Specifications.

2.2. Mathematical Model

The water flowing through the T-junction and Venturi metre can be thought of as an incompressible, steady flow, which is in accordance with mass and momentum conservation laws. Therefore, the continuity and the Navier-Stokes equations are included in the basic equations.

$$\frac{\partial u}{\partial x} + \frac{\partial v}{\partial y} + \frac{\partial w}{\partial z} = 0$$

Where u , v , w is the velocity components in x , y , z -direction, respectively.

$$\frac{\partial(\rho u)}{\partial t} + \nabla(\rho u U) = -\frac{\partial P}{\partial X} + \mu \nabla^2 u + F_x$$

$$\frac{\partial(\rho v)}{\partial t} + \nabla(\rho v U) = -\frac{\partial P}{\partial Y} + \mu \nabla^2 v + F_y$$

$$\frac{\partial(\rho w)}{\partial t} + \nabla(\rho w U) = -\frac{\partial P}{\partial Z} + \mu \nabla^2 w + F_z$$

When considering time (t), velocity vector (U), water density (ρ), fluid pressure (p), dynamic viscosity of water (μ), and forces in the x , y , and z directions (F_x , F_y , F_z) respectively, if the only mass force acting is gravity and the Z -axis is vertical, then $F_x = 0$, $F_y = 0$, and $F_z = -\rho g$.

2.3. Flow parameters and Geometry

The T-junction and Venturi meter are drawn using the Cartesian coordinate system presented in Fig 1. The diameter of the pipe used ($D = 0.025$ m), the origin of the coordinate system is located at the beginning of the throat section therefore the length of the throat section is from $(0 - 0.015$ m), the convergent section is from $(0 - -0.025$ m), the entrance section from $(- 0.025 - - 0.05$ m). As the figure 1 show the outline of the pipe design and dimensions parameters are marked.

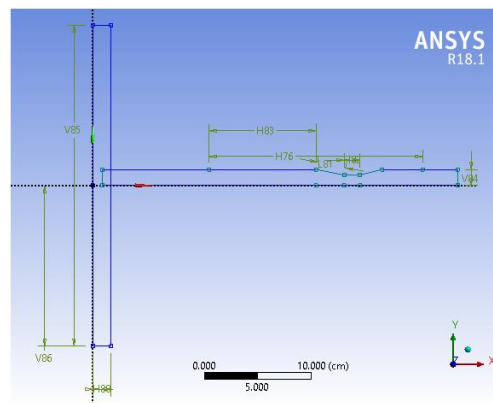


Figure.1. Dimensions of the pipe design

Dimensions: 19	
<input type="checkbox"/> A37	154.23 °
<input type="checkbox"/> A39	148.59 °
<input type="checkbox"/> A40	148.59 °
<input type="checkbox"/> A42	154.23 °
<input type="checkbox"/> H14	17 cm
<input type="checkbox"/> H18	17 cm
<input type="checkbox"/> H24	4 cm
<input type="checkbox"/> H29	1.5 cm
<input type="checkbox"/> H30	1.5 cm
<input type="checkbox"/> H43	5 cm
<input type="checkbox"/> H44	5 cm
<input type="checkbox"/> L26	2.7 cm
<input type="checkbox"/> L27	2.7 cm
<input type="checkbox"/> V13	13 cm
<input type="checkbox"/> V28	4 cm
<input type="checkbox"/> V4	13 cm
<input type="checkbox"/> V45	4 cm
<input type="checkbox"/> V7	15 cm
<input type="checkbox"/> V8	15 cm

Figure.2. Extruded 3d model design of the described dimension

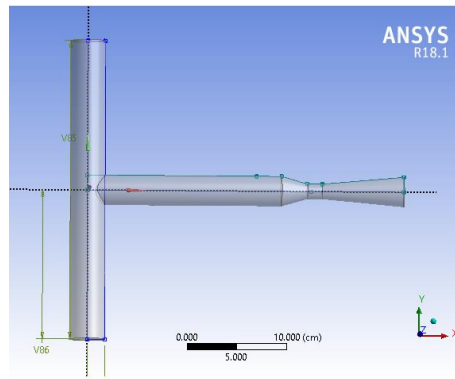


Figure.1. Selection and Boundary Conditions

2.4. Selection and Boundary Conditions

Within the computational domain, different parts or regions may be highlighted to represent selections. These selections could include specific surfaces, volumes, or components of the system that are of interest for analysis or have specific boundary conditions applied to them. For example, inlet and outlet surfaces, walls, or specific internal components may be selected for further analysis.

The figure would also illustrate the boundary conditions applied to different parts of the computational domain. This could include:

Inlet Boundary: Where fluid enters the domain. This might be indicated by an arrow or annotation indicating the direction and velocity of the incoming flow.

Outlet Boundary: Where fluid exits the domain. This might be depicted similarly to the inlet boundary.

Wall Boundary: Surfaces where fluid interacts with solid boundaries. These boundaries typically enforce a no-slip condition, meaning the fluid velocity at the wall is zero.

Symmetry or Periodic Boundary: Representing symmetry planes or periodic boundaries in the system, if applicable.

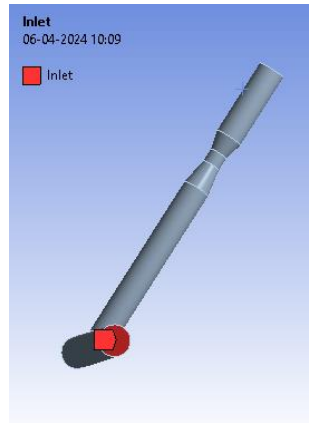


Figure.4. Represent the inlet section

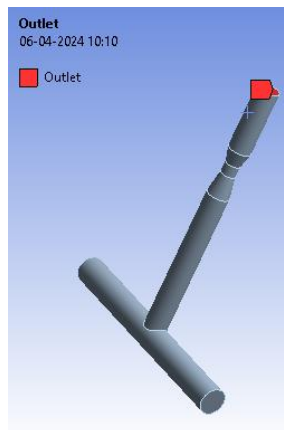


Figure.5. Represent the outlet section

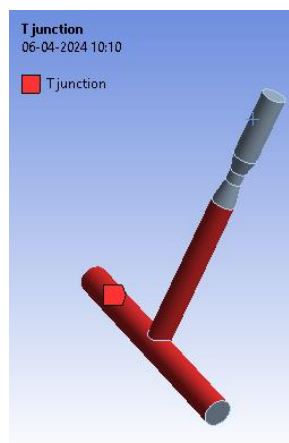


Figure.6. Represent the T-joint section

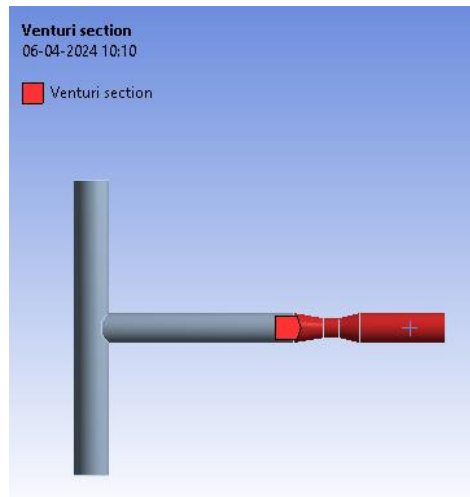


Figure 2. Represent the Venturi section.



Figure.3. Represent the wall of the pipe.

2.5. Simulation Parameters

The simulation employs water with a consistent density of 998 kg/m^3 and dynamic viscosity of 0.001 kg/ms . The fluid flow is assumed to be incompressible. Boundary conditions are established with a prescribed velocity at the inlet and zero initial gauge pressure. The velocity profile within the inlet pipe is considered fully developed. It is assumed that all walls adhere to a no-slip boundary condition. The simulation is conducted using ANSYS FLUENT 2018.1, a computational fluid dynamics (CFD) software. Employing the finite volume method and a first-order upwind difference scheme, the differential equations are transformed into algebraic equations. The coupling procedure is employed to calculate the pressure-velocity coupling of discrete

equations. The computational grid, depicted in Figure 2, is unstructured and comprised of 6805 nodes and 30468 elements, featuring five boundary layer cells with an element size of 0.5mm.

Statistics	
<input type="checkbox"/> Nodes	6805
<input type="checkbox"/> Elements	30468

Figure.4. Statistics

2.6. Mesh Analysis

Meshing process to calculate the point where the loads are applied. Contact region (input and output) flow and fluid domain are created. SIMULATION and FLUID FLOW (FLUENT) are used to mesh the solid and fluid domain, respectively. A fluent mesh analysis in workbench describes when the files that are generated and used by fluent meshing and the cell zones change as in T-joint through venturi section with a fluent component system in workbench. Basic fluid flow analysis starting from an imported mesh it is also possible to bypass the geometry cell, and begin the simulation process by importing a mesh Right click the mesh cell and select mesh file In the dialogue open, browse to find u-tube mesh file and select open There are three basic steps to creating a mesh: create geometry for the meshing application.

2.7. Solution and Methods

Turbulent steady-state flow conditions were meticulously simulated using ANSYS Fluent, a renowned computational fluid dynamics software. The study focused on a robust solution methodology to accurately depict the intricacies of turbulent fluid dynamics. Utilizing the finite volume method, the governing equations, including the Navier-Stokes equations, were discretized to capture the turbulent flow phenomena within the computational domain. For turbulence modeling, the widely adopted k-epsilon model was employed, with parameters set to typical values of turbulent kinetic energy (k) at $0.01 \text{ m}^2/\text{s}^2$ and dissipation rate (epsilon)

at $0.1 \text{ m}^2/\text{s}^3$. The pressure velocity coupling algorithm ensured convergence to a steady state, with a convergence criterion set at 10^{-6} for the residual values. Through meticulous iterations, the simulation accurately depicted the turbulent flow behavior, shedding light on its complexities and providing valuable insights for various engineering applications.

2.8. Setup and post process

The boundary condition is given for inlet in terms of pressure. After which the solution of the flowmeter was calculated. The solution gives the graph between the iteration and the flow of the pipe in continuity and in X, Y, Z velocity it is repeated for 500 iteration of the flow. Setup and solution procedure is followed by mesh file into ANSYS fluent and setup u-tube model. The solution cell contain u-tube general properties and some specific properties related to the solution process. The solution controls for the solver are populated with default settings and values. Fig.10 shows the flow rate vs iteration.

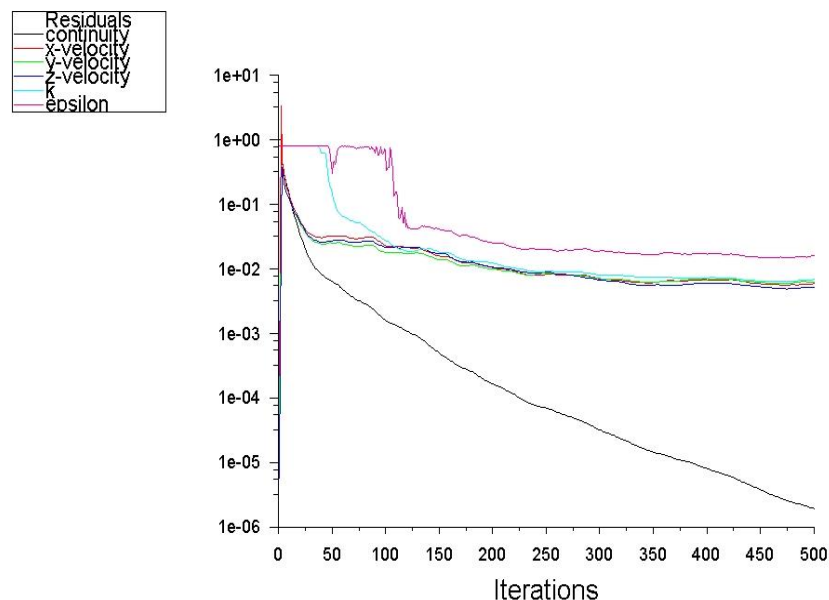


Figure.5. Flow versus iteration

3. Result and Discussion

Following the design, simulation, and post-processing stages of the T-joint Venturi meter project, the results unveiled significant insights into the fluid flow dynamics. Streamline visualization illustrated how fluid particles traversed the system, showcasing acceleration as they passed through the Venturi throat. Velocity distribution plots confirmed this acceleration, with higher velocities near the throat and lower velocities elsewhere. Pressure contour plots highlighted regions of high and low pressure, with the lowest pressure occurring at the Venturi throat, aligning with Bernoulli's principle. These findings were crucial for understanding energy losses and flow resistance within the system, aiding in its optimization. Additionally, comparison with theoretical and experimental data validated the simulation model, ensuring its reliability for future applications.

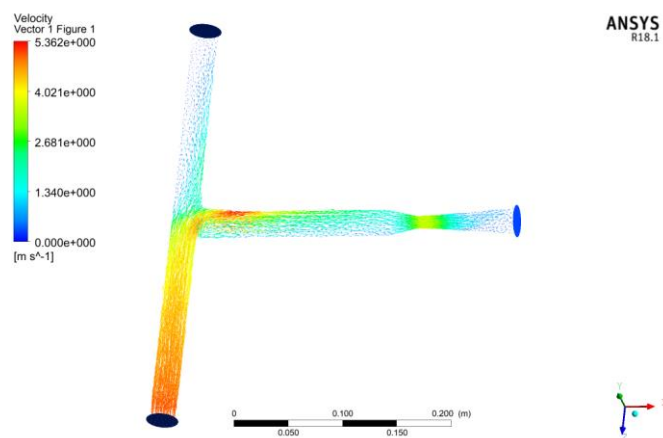


Figure.6. Velocity distribution among the design of the specified conditions

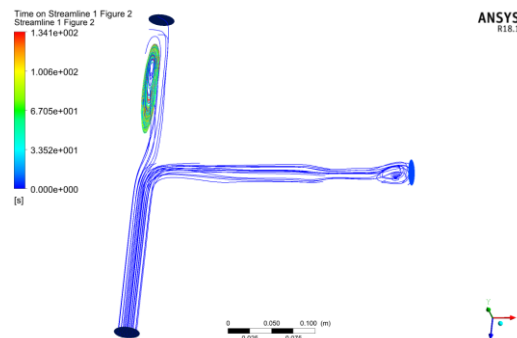


Figure.7. Flow of the fluid behavior through the pipe

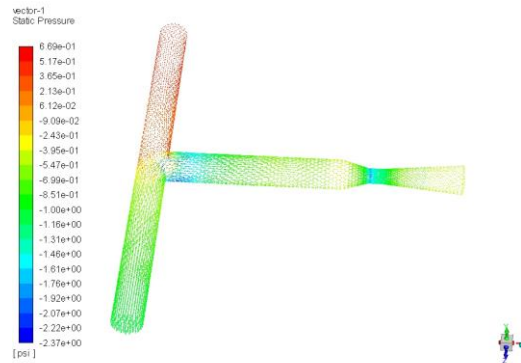


Figure.8. Static pressure distribution during the flow

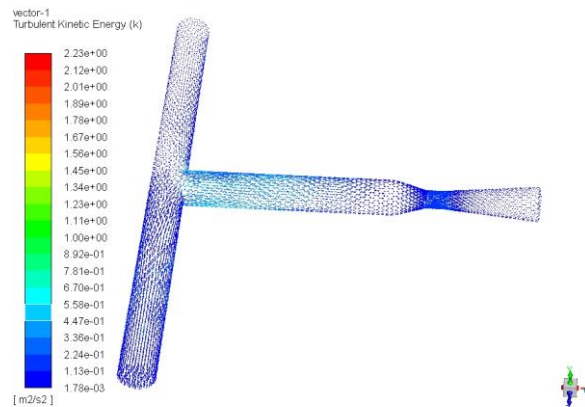


Figure.9. Turbulence behavior of the fluid during the flow

4. Conclusion

The reaction of the Venturi meter design to simulation parameters reveals critical insights into its performance characteristics. Alterations in parameters such as inlet velocity, throat diameter, and pipe dimensions directly shape the flow behavior within the meter. Higher inlet velocities accentuate pressure drops and enhance flow rate accuracy, while adjustments to the throat diameter directly impact velocity profiles and pressure distributions. Furthermore, variations in pipe dimensions introduce changes in flow patterns, turbulence levels, and energy losses, underscoring the importance of meticulous consideration during design and

simulation phases. Through systematic adjustment and scrutiny of these parameters in simulations, a comprehensive understanding of the Venturi meter's behavior can be achieved. This knowledge facilitates optimization and enhances the meter's performance in real-world applications, ensuring accurate and reliable flow measurement.

REFERENCES

- [1]. Benjamin G. Sandberg, "Venturi Flowmeter Performance Installed Downstream Of The Branch Of A Tee Junction," 2020.
- [2]. J. Clerk Maxwell, *A Treatise on Electricity and Magnetism*, 3rd ed., vol. 2. Oxford: Clarendon, 1892, pp.68–73.
- [3]. C. Sanghani and D. Jayani, "Optimization of Venturimeter Geometry for Minimum Pressure Drop using CFD Analysis," vol. 3, no. 2, pp. 31–35, 2016.
- [4]. H. Reza and M. Reza, "Optimizing Different Angles of Venturi in Biodiesel Production Using CFD Analysis," vol. 38, no. 6, pp. 285–295, 2019.
- [5]. Akeel M. Ali Morad, Rafi M. Qasim, Amjed Ahmed Ali, *Study of the behaviours of single-phase turbulent flow at low to moderate reynolds numbers through a vertical pipe. Part i: 2d counters analysis*, 2020.
- [6]. M. F. P. N. P. Costa, R. Maia, F. T. Pinho, "Edge Effects On The Flow Characteristics In A 90° Tee Junction," pp. 1–44, 2006.
- [7]. Bhatkar MR, Ban PV, *Review Study on Analysis of Venturimeter using Computational Fluid Dynamics (CFD) for Performance Improvement. in International Research Journal of Engineering and Technology (IRJET)*. 6: 226-228, 2019.
- [8]. M. S. Shah, J. B. Joshi, A. S. Kalsi, C. S. R. Prasad, and D. S. Shukla, "Analysis of flow through an orifice meter: CFD simulation," *Chem. Eng. Sci.*, vol. 71
- [9]. K. V. Santhosh and B. K. Roy. (2012). *An Intelligent Flow Measuring Technique Using Venturi*. Proceedings of International Multi-Conference of Engineers and Computer Scientists, Vol. II., pp. 300–309, 2012.
- [10]. Denghui He, Senlin Chen, and Bofeng Bai, *Experiment and Numerical Simulation on GasLiquid Annular Flow through a Cone Sensor*, *Sensors*, 18(9): 2923, 2018.
- [11]. He D.H., Bai B.F., Wang X.W. *Online measurement of gas and liquid flow rate in wet gas through one V-Cone throttle device*. *Exp. Therm. Fluid Sci.* 2016;75:129–136.